Proceedings of ASME Turbo Expo 2011
GT2011
June 6-10, 2011, Vancouver, British Columbia, Canada

GT2011-46415

LES AND RANS ASSESSMENT OF RIB COOLED CHANNEL RELATED TO SGT-800 COMBUSTOR LINER

Daniel Lörstad
Siemens Industrial Turbomachinery AB,
SE-612 83 Finspong, Sweden

ABSTRACT

The main parts of the annular combustor liner walls of the Siemens gas turbine SGT-800 are convectively cooled using rib turbulated cooling. Due to the serial system of cooling and combustion air there is a potential of further reduction of total combustor pressure drop by improvements of the cooling system. Apart from the rib cooling, also the cooling channel bypass entrance is related to a significant part of the total cooling system pressure drop.

In this study, an investigation is performed for a rib cooled channel which is related to the considered combustor liner and where empirical correlations are available in order to evaluate the methodology used. The study includes an assessment of the Reynolds Averaged Navier-Stokes (RANS) and Large Eddy Simulation (LES) models available within commercial Computational Fluid Dynamics (CFD) codes and includes also an investigation of model size when using periodic boundaries for LES simulations. It is well known that a small geometrical distance in the direction of the periodic boundaries may have a strong effect on the flow field but is often neglected in practice in order to speed up LES calculations. Here the effect is assessed in order to show what size is required for accurate results, both for time averaged and transient results. In addition too small domains may be affected by spurious low frequencies originating from the periodic boundaries requiring additional simulation time for time converged statistics, but also the averages may be significantly affected. In addition the simulation period for time converged statistics is evaluated in order to show that larger model size in the periodic direction does not necessarily require longer practical simulation time, due to the fact that larger volumes may be used for the combined time and space averaging. The aim is to obtain practical guidelines for LES calculations for internal cooling flows. Then the study is extended step by step to investigate the importance due to high Reynolds number, variable fluid properties and large temperature gradients in order to cover the ranges and specifics required for SGT-800 engine conditions.

NOMENCLATURE

AR	Aspect ratio: Width/Height
A_c	Cross area [m^2]
A_w	Wall surface area [m^2]
α	HTC: $Q=\alpha A_w\|T_w-T_f\|$
CFD	Computational Fluid Dynamics
CFL	Currant-Friedrichs-Lewy number = $U^*\Delta t/\Delta x$
CHT	Conjugate Heat Transfer
D_h	Hydraulic diameter =4*area/perimeter [m]
DLE	Dry Low Emissions
Δt	time step size [s]
Δp	Pressure drop [N/m^2]
Δx	Cell size in flow direction [m]
e	Rib height [m]
f	Friction factor: $\Delta p/L^*8D_h/(\rho U^2)$
f_0	Smooth wall f: $0.331/[\ln(5.74/Re^{0.9})]^2$
HTC	Heat Transfer Coefficient: α [W/m^2K]
L	Channel length [m]
λ	Thermal conductivity [W/mK]
LES	Large Eddy Simulation
PLC	Pressure Loss Coefficient: $2\Delta p/(\rho U^2)$
Nu	Nusselt number: $\alpha D_h/\lambda$
Nu_0	Smooth wall Nu: $0.023^*Re^{0.8*}Pr^{0.4}$
μ	Dynamic viscosity [kg/ms]
P	Pitch (distance between ribs) [m]
Q	Heat transfer [W]
RANS	Reynolds Averaged Navier-Stokes equations
RSM	Reynolds Stress turbulence Model
ρ	Density [kg/m^3]
Re	Reynolds number: $\rho UD_h/\mu$
SGT	Siemens Gas Turbine
SST	Shear Stress Transport (turbulence model)
T_w	Wall temperature [K]
T_f	Flow bulk temperature [K]
TBC	Thermal Barrier Coating
TIT	Turbine Inlet Temperature [K]
U	Bulk velocity [m/s]

INTRODUCTION

The efficiency and power output of a gas turbine increases with higher turbine inlet gas temperature. Modern gas turbines are exposed to hot gases of temperatures that far exceed the melting point of the component material and thus have to be cooled. When cooling the component it is important to accurately predict the cooling efficiency and distribution, to avoid local high wall temperatures that may cause issues of TBC flaking or metal oxidation. It is also important to avoid large temperature gradients that may cause thermal stresses leading to reduced component life or local over-cooling, that indicates that the pressure drop or cooling mass flow may be reduced.

Convective cooling may be improved using turbulated ribs, where the heat transfer is increased by enhancement of the flow turbulence and by breaking the boundary layer. The penalty for the increased heat transfer is higher pressure loss. The methodology is common for gas turbine vanes and blades due to the high cooling efficiency and reasonable manufacturing process and cost, where the rib turbulated cooling is typically used in the leading edge or mid region of the airfoil. Maximum cooling with minimum cooling air is desired, since the extraction of cooling air decreases the efficiency of the turbine due to less air available for power generation. It also reduces the amount of combustion air available, which may limit DLE combustor performance.

Rib turbulators are also common for combustor liners, where the air extracted from the compressor is used for combustor cooling and combustion in either a serial or parallel manner. For the serial approach, the combustor air is used to cool the liners before entering the burners and hence the combustor pressure drop is the sum of the cooling part and the combustion part. The main advantage is that TIT may be as high as the flame zone temperature which is limited for DLE combustion systems. For the parallel approach the cooling and burner air enters the combustor through separate passages of similar pressure drop. Unless the cooling air is well mixed into the flame zone of the combustion chamber, the corresponding flame temperature will be higher than TIT. Hence combustor cooling efficiency development work for the serial approach is focused on pressure reduction using large amount of air, while for the parallel approach the focus is on cooling air flow reduction at specified pressure drop and increased mixing of cooling air into the flame zone.

In this work the focus is on the SGT-800 combustor liner cooling, which uses the serial cooling approach. The combustor is shown in Figure 1, where the main flow paths, the flame and the main combustion recirculation zones are shown. The SGT-800 is the largest industrial gas turbine manufactured by Siemens Industrial Turbomachinery AB (SIT) and is produced in Finspong, Sweden. The gas turbine ISO rated power range is up to 47MW using 37.5% single cycle efficiency [1, 2].

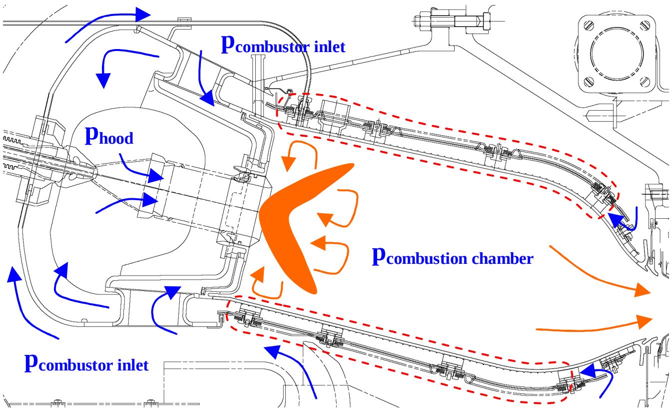

Figure 1: SGT-800 annular combustor: Main flow paths, recirculation zones and liner regions.

The annular combustor is convection cooled and hence nearly all combustor air is used for the combustion, allowing for almost equal flame zone temperature as for TIT. This is an advantage for DLE combustion system, allowing for relatively high TIT using relatively low flame temperature. The annular concept also yields a relatively smooth tangential TIT and reduced cooling surface area to combustor volume ratio compared with a can system. The combustor is recently improved using passive acoustic damping and an improved impingement cooling system of the front panel heat shield [3]. Figure 1 shows the location (marked in red) of the outer and inner liners which are the focus in this study.

The cooling of the liners involves a high Reynolds number flow of the order of 200k-300k, one sided 90 degree rib cooling in a wide channel of varying height, e/D_h~0.028-0.038, P/e~10, large temperature gradients affecting the fluid properties, conjugate heat transfer, corner sharpness affected by production tolerances and curved surfaces in both axial and tangential direction. Much work of the efficiency of rib turbulators has been performed in the open literature and most is performed with the aim of improved prediction for vanes and blades. Therefore the main focus in general has been the cooling in channels of constant height, aspect ratios of 0.25-4, rib angles of 30-90 degrees and Re below 100k. An overview of the performed measurement work and correlations that are most appropriate for gas turbine rib cooling has been performed at Siemens by Sundberg [4], and the outcome of the study is that the four correlations developed by Han and co-workers [5-8] are recommended. However, many uncertainties remain and the different correlations show quite large differences within their respective valid ranges. The most important factor missing within these correlations is the effects due to high Re. This includes for example the value of P/e~10 which is considered optimal but may have to be adjusted for higher Re since the flow attachment downstream the ribs is significantly closer for higher Re. For Re=60k the flow reattaches ~2 rib heights downstream compared to 6 rib heights for Re=10k [5].

Rallabandi et al. [9-10] studied Re up to 400k for 45 degree ribs and showed that the heat transfer performance reduces with Reynolds number due to a reduction in Nusselt number ratio to non-ribbed channels. The friction factor was shown to be constant with Re but strongly non-linearly dependent with rib height, indicating that ribs of e/D>0.1 suffer from significantly increased losses [9]. Corner sharpness has been addressed and the effect is minor, however, there is still uncertainty of how to apply the results to the empirical correlations [10]. The high Re trends for 90 degree ribs have been investigated by Kunstmann et al. [11] and Hagari et al. [12] for a certain choice of geometry. However, so far the investigation for high Re is limited.

There are also plenty of examples of rib prediction using CFD. Chen et al. [13] used RANS SST for rib predictions and the results for 45 degree ribs show reasonable agreement to experiments but for 90 degree ribs the deviation is significant. The reattachment point is predicted too far away from the upstream 90 degree rib which results in a significant under prediction of the heat transfer and friction factor since the reattachment point corresponds to the peak heat transfer. Zehnder et al. [14] also simulated 45 degree ribs and stated that both k-epsilon realizable and SST models resulted in reasonable accuracy for a straight square channel.

The conclusion is that RANS models seem to have large difficulties predicting 90 degree ribs obtaining the same accuracy as for <60 degree ribs. LES have the potential of improved accuracy at the cost of computational resources, which is proven by a number of investigations [15-20]. However, these investigations include a single or a few test cases each and due to the scatter in the results due to the different correlations available, more work is required to evaluate how LES is best applied to rib cooling, in order to obtain sufficient efficiency and accuracy.

Since semi-empirical correlations are obtained for certain lab models including limitations in geometry, boundary specifications and flow ranges, there are often differences to the real engine case. Hence there is a need for complementary experiments for a certain case to be valid or to reliably quantify the effect of a modification which is outside the valid range of the correlation. CFD has the potential to close such a gap, but in order to be reliable the trends must be verified. Most investigations use CFD to study a limited number of cases where they complement the performed experiments with detailed data that are not easily measured. An accuracy level of similar size as the experiments (<10%) is usually acceptable, however, there is a risk that the accuracy is worse for a modified case and hence that the trends have larger errors than the evaluated case or cases. In order to use CFD to extend the valid range of a correlation, the trends must be investigated thoroughly. For 90 degree ribs this must most likely be performed using LES due to the lack of performance for RANS. Such an assessment requires a certain accuracy of the results, which includes reasonable convergence of cell size, time step and simulation time. Also the geometrical model size must be verified since LES accuracy may be strongly affected by the boundary conditions if the model is selected too short in the flow direction or too thin in transversal direction. This is often neglected due to computational cost and due to the assumption that the error is small even though it may not be negligible. Here is presented such an approach with the overall goal of verifying the trends of RANS and LES predictions, in order to find a reliable tool that may be used to extend existing correlations with sufficient accuracy to be applicable for SGT-800 liner cooling.

90 DEGREE RIBS IN A WIDE CHANNEL

Due to the annular combustion chamber of SGT-800, the rib cooled liner cooling channels are cylindrical of high radius compared to the channel height. Therefore the cooling channels may be approximated with a straight wide channel for a basic investigation. Most previous investigations focus on channels of limited width and usually W/H≤4. For high Re≥100k the number of previous investigations are even more scarce, but a summary of the results for 1-sided ribs of Kunstmann et al [11] of AR=2 and e/D_h=0.02 and the results from Hagari et al [12] for AR=4.375 and e/D_h=0.01 are shown in Figure 2. Their results are compared to the empirical correlations of (1) Han [5] that is valid for 2-sided ribs, 10k≤Re≤60k, AR≤4, 10≤P/e≤20 and 0.05≤e/D_h≤0.08, (2) Han & Park [6] that is valid for 2-sided ribs, 10k≤Re≤80k, AR≤4, 10≤P/e≤20 and 0.02≤e/D_h≤0.08 and (3) Chandra et al [8] that is valid for 1-4 sided ribs, 10k≤Re≤80k, AR~1, P/e=8 and e/D_h~0.06. It should be noted that neither of these correlations are applicable for Re>80k or very high aspect ratio but due to the lack of valid correlations for high Re the correlations are extended for comparison using dotted lines and symbols. As clearly seen, there are relatively large differences both between the different correlations and to the measurement data, and especially for the low Re range. The differences between the correlations may be at least partly explained that they are used outside their valid ranges. At least the results of the measurement data confirm that the heat transfer Nu/Nu_0 is rather constant with Re for Re≥100k.

The difficulty of trend prediction is shown in Figure 3, where the results from both measurement data sets are combined together with the correlation of Chandra et al. [8] for both Nu and friction factor ratio. The measurement data shows that the friction factor f/f_0 is slightly increasing after Re>100k. Since the measurement data is using different AR and e/D_h these effects are separated using the correlation, where it is shown that increased e/D_h and AR increases both Nu and f. The differences between the measurement cases are much larger than the estimated differences due to AR and e/D_h according to the correlation. This may be due to different types of errors in the different measurement setups or due to limited accuracy for the empirical correlation for this setup of geometrical data, which leads to the conclusion that more work has to be performed to close these question marks. It also emphasizes the importance of improving the accuracy of prediction tools, such as CFD, as an alternative way to answer such question marks.

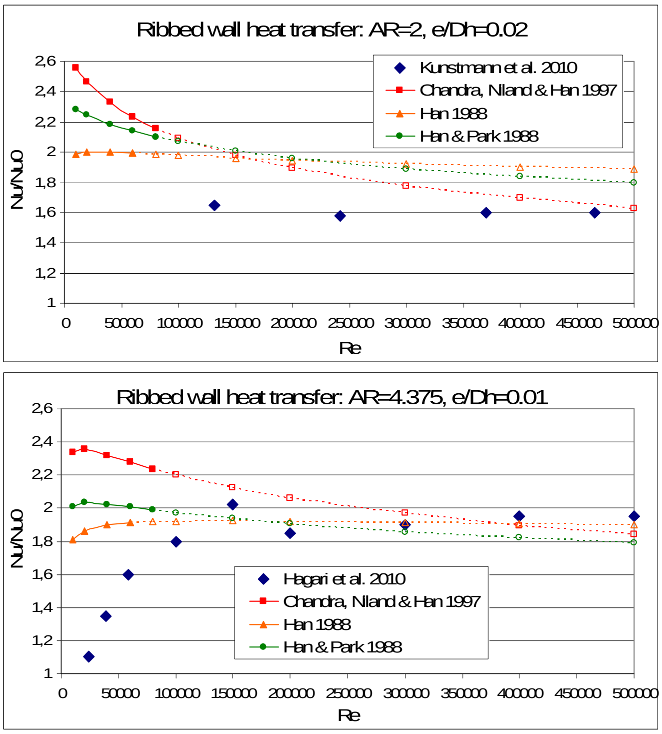

Figure 2: Nusselt number using different references [5-6,8,11-12]. The data are scaled with smooth wall data.

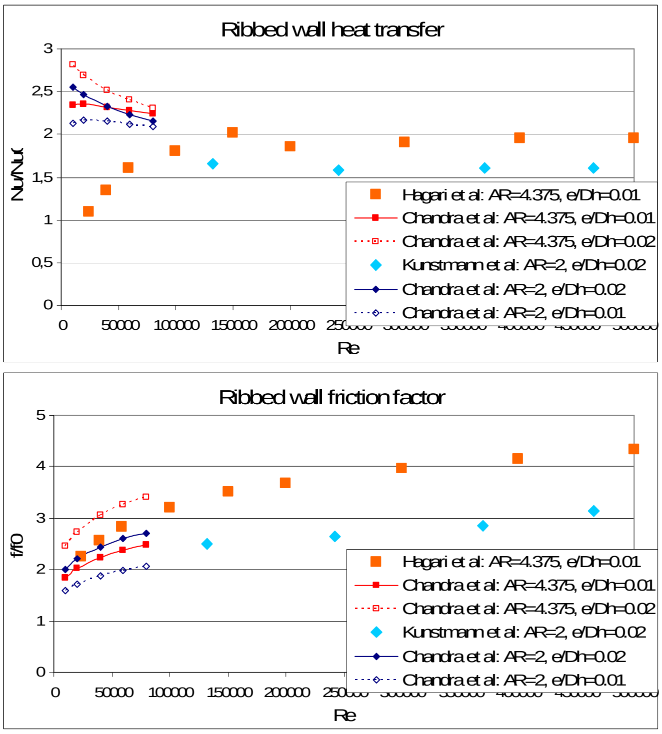

Figure 3: Nusselt number and friction factor using different references [8,11-12]. The data are scaled with smooth wall data.

COMPUTATIONAL MODEL

A straight wide channel with 2-sided 90 degree ribs is selected as the main evaluation case, which is similar to the square case used by Sundberg [3]. This test case has similar e/D_h and P/e as the SGT-800 liners, as shown in Table 1.

An unstructured hexahedral mesh corresponding to this geometry is obtained using Ansys Gambit. Figure 4 shows the grid in the vicinity of the ribs, where the boundary layer is attempted to be resolved. In transversal direction the grid is equally spaced.

Table 1 summarizes the geometry, mesh and boundary condition data for Grid 1. In order to investigate the influence of the periodic boundary conditions that is applied in both the streamwise and transversal direction, the model is created using different values for channel length L/P and width W/H. To fulfill thermal periodicity opposite heat transfer boundary conditions are applied for the ribbed walls, i.e $-Q_{lower\_wall}= Q_{upper\_wall}$. Unless otherwise specified, constant fluid properties are used for air at 25C at atmospheric conditions.

This case may be efficiently simulated using LES since the model is compact, i.e. a relatively small number of time steps are required per flow through time. In addition a 2-sided ribbed wall using inverse thermal boundary conditions will yield symmetry for the heat transfer distribution of the opposite walls, and hence the required simulation time for sufficient time convergence may be reduced.

The software ANSYS Fluent 12.0 is used for all simulations. Incompressible flow, constant properties and the standard settings for the corresponding solver are used unless otherwise specified. The Fluent cases involve both RANS and LES simulations using different turbulence models [21]. The discretization scheme is second order for all variables and for all cases in both space and time; however, the spatial discretization is bounded central differences for LES and second order upwind for RANS.

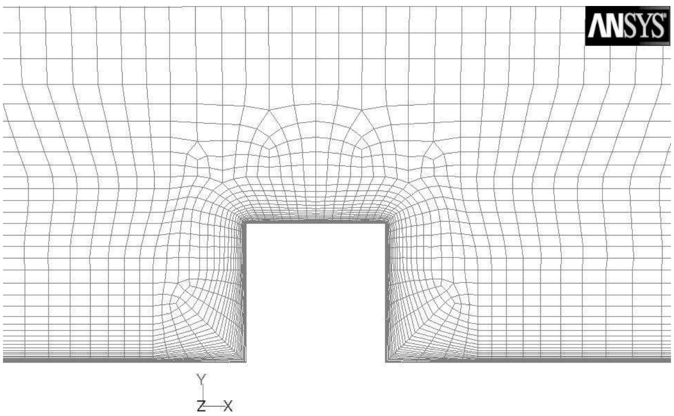

Figure 4: Mesh in the vicinity of the rib for Grid 1.

Table 1: Data for ribbed channel.

P [mm]	3.15
H [mm]	5
D_h=2H [mm]	10
P/e	10
e/D_h	0.0315
W/H	0.4 - 2.4
L/P	1 or 2
# ribbed walls	2
Alfa [o]	90
Re	10k-500k
$Q_{lower\ wall}$ [W/m2]	10k
$Q_{upper\ wall}$ [W/m2]	-10k
$T_{inlet\_average}$ [K]	298
# cells for L=P & W/H=1.2	0.5 M hex for Grid 1

RANS investigation

Firstly is presented an investigation using RANS as shown in Figure 5, where the heat transfer and friction factor due to Re are shown. The empirical correlations [5-6,8] are shown for comparison, despite the question marks in previous section. The correlations are limited to AR≤4 and Re<80k but to estimate the effect of wider channels they are extrapolated to AR=100 for comparison. Note that filled lines show the correlations reasonably within the valid range and dotted lines show extrapolated data. The RANS results are similar between k-e Realizable and RSM for both Nu and f, but there are huge differences of the levels compared to SST even though the basic trends are similar. All tested RANS models show that Nu/Nu_0 is increasing with Re, which is not supported by the correlations. Therefore there are question marks whether RANS can be used to predict trends, or if the correlations show the correct behavior since they are extrapolated to AR=100. To verify the grid independency of the RANS results, adaptive grid refinement of all cells was applied to the cases of Re=230k which affected the results ~1%.

LES investigation

Simulations using LES in general require a vast amount of computational resources. In order to minimize that, the most efficient model is sought, where efficiency is defined as maximum accuracy for a certain amount of computational effort. This is performed by investigating the accuracy reduction due to different simplifications, one at a time. This involves the required time step, total simulation time for averaging, geometrical model size, boundary conditions, LES sub-grid scale model and grid size. By comparing the introduced error to saved simulation time for each simplification, the optimum model may be found.

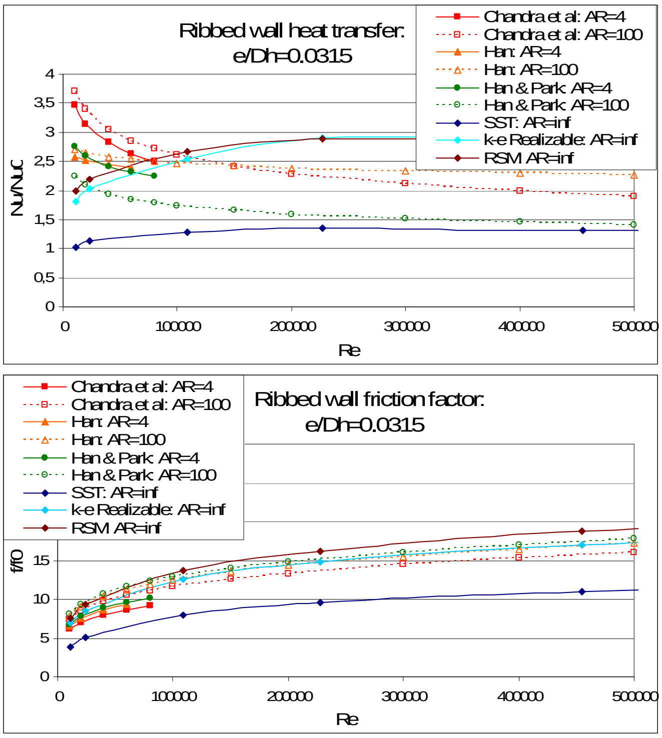

Figure 5: Nusselt number and friction factor using different RANS models and correlations [5-6,8]. The data are scaled with smooth wall data.

Both constant pressure drop and mass flow conditions have been applied. However, due to difficulty to extract the time dependent pressure drop from Fluent, the time averaged friction factor is only calculated for cases using constant pressure drop conditions.

First the dependency due to total simulation time, time step size and geometrical model size is investigated using the standard Smagorinsky SGS-model. The model was chosen for stability reasons and due to the assumption that the SGS-model should not strongly influence the required model size or time step size.

Figure 6 shows the results for heat transfer and friction factor for Re~24k and different CFL-number, where the CFL is defined by the bulk velocity and the streamwise cell size at the middle of the channel. This CFL is typical for most of the cells, however, the max CFL number is about 20 times larger, based on the local cell velocity and flow direction cell size. A CFL number around one means that a fluid particle would travel through a numerical cell in one time step. If CFL is much larger than one, then the smallest vortices would be damped which may affect the LES accuracy negatively and therefore the effect of CFL is thoroughly investigated. In addition the simulation time is verified to be sufficient for all cases. The results show that both Nu/Nu_0 and f/f_0 are in general reducing with time step size. When comparing the geometrical sizes, it is noted that the channel width has a strong influence since W=0.4H results in much lower heat transfer and friction factor. It is worth emphasizing this result since there are many examples in the open literature where thin LES models are used without investigating the effect of channel width. However, the differences between W=1.2H and W=2H is small in comparison, so the conclusion is that W≥1.2H seems sufficient. When amplifying the geometrical size further using double length in both streamwise and transversal direction, i.e. L=2P (2 ribs) and W=2.4H, the results are somewhat but much less affected confirming that further geometrical model expansion is not critical. The bump at CFL~0.5 is explained by a very low frequency content that only occurs for some cases for the smaller models, which significantly affects the averaged results and amplifies the required total simulation time. In order to investigate if this low frequency content is due to the use of constant pressure drop boundary conditions that allows for mass flow fluctuation, the constant mass flow conditions were confirmed to yield similar results. This is to be further discussed in Figure 8.

Figure 7 shows the corresponding results for Re~230k which confirms similar trends as for lower Re even though the variation between cases are somewhat smaller than for the lower Re case.

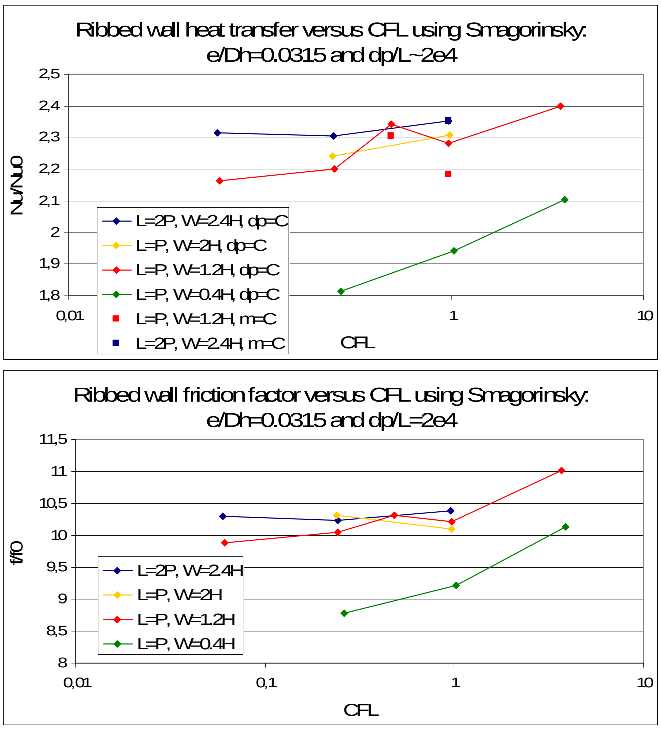

Figure 6: Ribbed wall heat transfer (top) and friction factor (bottom) for LES standard Smagorinsky model at Re~24k for different mesh sizes and time steps.

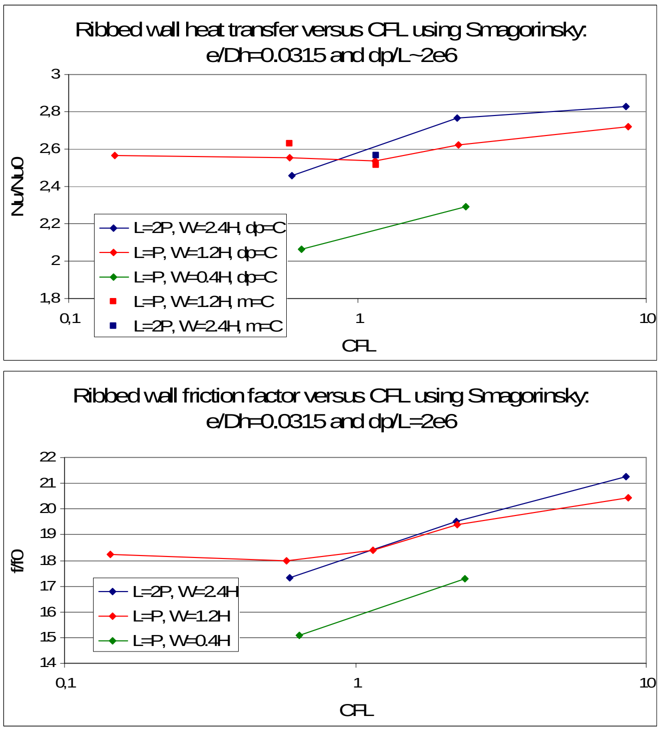

Figure 7: Ribbed wall heat transfer (top) and friction factor (bottom) for LES standard Smagorinsky model at Re~230k for different mesh sizes and time steps.

Table 2 shows the results for different LES models at different Re, where the dynamic Smagorinsky and Wale models [21] are added to the comparison using L=P and W=1.2H using constant pressure drop boundary condition. The results show that the standard Smagorinsky model results in an unrealistic increase in Nu/Nu_0 for higher Re while the dynamic Smagorinsky and Wale models show similar trends, which both seems realistic compared to Figures 2, 3 and 5. The Wale model was selected for further studies since it is somewhat faster and seemed to suffer slightly less from the low frequency content as compared to the dynamic Smagorinsky model.

Table 2: Ribbed heat transfer and friction factor for e/D_h=0.0315, L=P, W=1.2H and CFL~1.

SGS-model	kRe	Nu/Nu0	f/f0
Smagorinsky standard	24	2.28	10.2
Smagorinsky dynamic	24	2.33	10.5
Wale	24	2.21	10.1
Smagorinsky standard	230	2.54	18.4
Smagorinsky dynamic	230	2.17	18.8
Wale	230	2.15	18.9

In order to show an example of the effect of the low frequency content, Figure 8 shows the Wale simulation of L=P and W=1.2 using both constant mass flow and constant pressure drop conditions. The time axis is scaled with the averaged streamwise velocity and the channel length to show the huge number of flow through times required obtaining reasonable time averages. The transient heat transfer for this case for the constant mass flow condition shows much more low frequency content than the case using constant pressure drop, but note that this is not always the case. The case using constant pressure drop on the other hand has significant variations (±4%) of the total mass flow, which decreases with larger model size (about ±1% for L/P=2 and W/H=2.4). However, the transient variation in mass flow is not strongly connected to the variation of heat transfer as shown in the upper figure, where Nu_0 is estimated using the averaged mass flow from the whole simulation. Since the total mass flow is included in the estimation of Nu_0 the final accuracy of Nu/Nu_0 is dependent on both the averages of heat transfer and mass flow. In general time converged Nu/Nu_0 may be obtained using shorter simulation time using constant mass flow conditions, however, the model size must be sufficiently large to avoid spurious low frequencies. In addition the period of time to stabilize the flow up front time averaging is significantly shorter using mass flow condition.

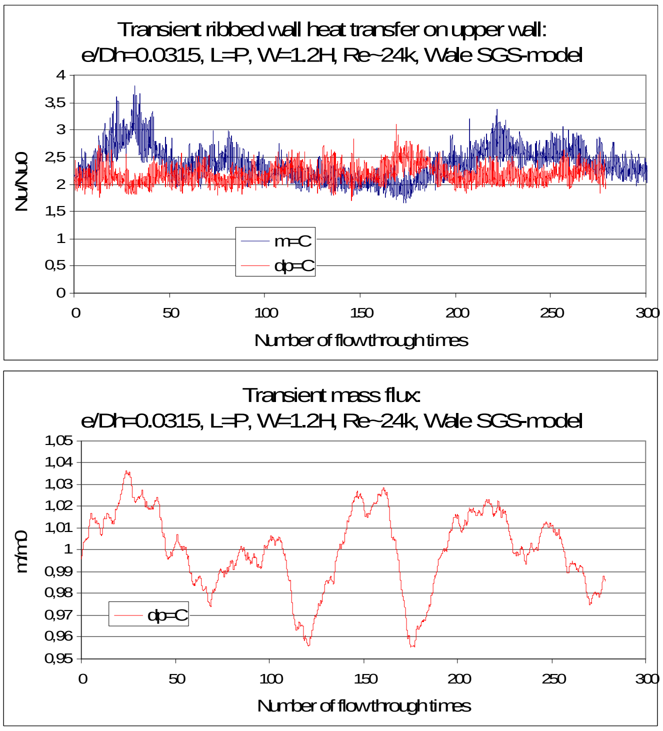

Figure 8: Transient ribbed wall heat transfer on upper wall for constant mass flow and constant pressure drop using Wale SGS-model and CFL~1.

The next step is to make sure of reasonable grid dependency, which has been performed using mesh refinement as shown in Table 3. Since grid dependency in general is more difficult to obtain for higher Re, the focus is on the Re=230k case. All tests are compared to their corresponding reference test without any refinement. The first test was performed by splitting all cells in all directions within 2e distance from the walls in order to investigate the grid dependency of Grid 1. The difference in the results of averaged Nu were significant (~10%) and therefore the conclusion is that Grid 1 have to be improved. In order to make sure how the grid should be refined without wasting unnecessary cells, several refinement tests were performed using smaller geometrical domains for faster analysis. The same initial field was used for all refinement tests and the simulations were stopped after a limited number of flow through times (as shown in the table) in order to avoid the growth of potential spurious low frequencies. Therefore the results of tests 2-8 are not fully time converged, even though the trends are clear.

The second and third refinement tests confirm that the main source of grid independency is within the close region of the ribbed walls, since the results are similar when refining all the domain (i.e. 8 times more cells) as compared to 2e from the walls. The fourth test used a refinement in between e/2 and 2e from the walls, i.e. at the rib tip and in the shear layers behind the tips but not at the wall in between the ribs, which resulted in a very similar transient behavior as for the non-refined reference case. This indicates that the main source of grid independency is located at the walls in between the ribs. The fifth test using refinement of the cells closest to the walls also show a significant difference. The sixth test using double number of cells only in the transversal direction show almost as large effect as global refinement. Therefore the conclusion is that Grid 1 has to be significantly refined in transversal direction and somewhat in the streamwise direction within the boundary layer, which resulted in Grid 2 as shown in Figure 9. Grid 2 uses more than 5 times more cells than Grid 1, which results in 10.7M cells for L=2P and W=2.4H. The wall normal resolution is similar between Grid 1 and 2, which is assumed sufficient since the instant y+ field for Re=230k is <1.2 as shown in Figure 10. The highest y+ values are found at the inward front corners of the ribs, since for mesh quality reasons the first cell layer is thicker at the inward corners, as can be seen in Figures 4 and 9. The rib tip experiences y+<0.9, however, due to a cell thickness to transversal width ratio of ~200 this results in z+<180 for Grid 2 and approximately 5 times higher for Grid 1. In between the ribs y+<0.35 is valid for most parts which together with cell thickness to length ratios of ~150 and ~100 in streamwise and transversal direction respectively results in x+<50 and z+<30 for Grid 2, while Grid 1 has about double x+ and about 5 times higher z+. The last three refinement tests in Table 3 confirm the grid independency improvement of Grid 2 compared to Grid 1.

Table 3: Nu Grid sensitivity study for e/D_h=0.0315, Re=230k (dp/L~2e6), Wale SGS-model and CFL~1.

Test	Grid refinement	W/H	L/P	FFT	%
1	Grid1: 2e from walls	2.4	2	>10	9.7
2	Grid1: all	1.6	2	4	9.3
3	Grid1: 2e from walls	1.6	2	4	9.5
4	Grid1: e/2-2e from w.	1.6	2	4	-0.4
5	Grid1: first 10 cells	1.6	2	4	6.1
6	Grid1: double in z	1.6	2	4	8.3
7	Grid1: all	0.6	1	4	12
8	Grid2: all	0.6	1	4	3.5
9	Grid2: all (86M cells)	2.4	2	>10	4.3

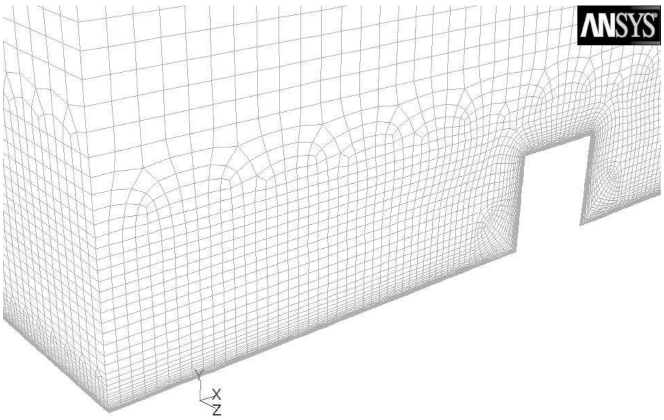

Figure 9: Mesh at the vicinity of the wall for Grid 2.

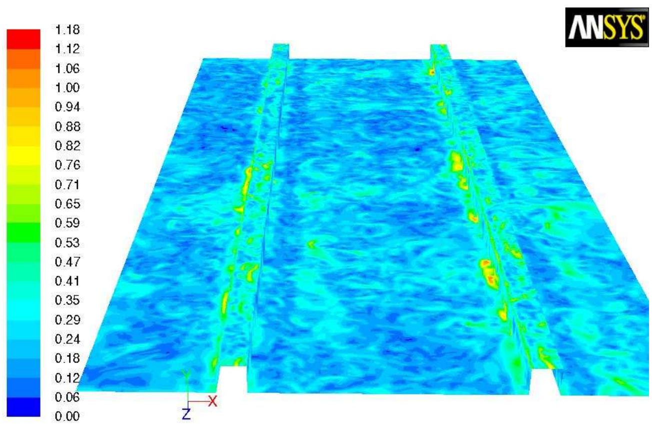

Figure 10: Instant y+ when using Grid 2, Re=230k , Wale SGS-model, L/P=2 and W/H=2.4.

Since L=2P and W=2.4H seem to be required for both model size independent results and to avoid spurious low frequencies, additional simulations using Wale and both Grid 1 and Grid 2 were performed as shown in Figure 11. The figure shows that the results converge rapidly with time step size for CFL≤1, which indicate that a global CFL~1 is a reasonable limit for accurate predictions even though this means a significantly higher CFL_{max}. The difference between Grid 1 and 2 is significant for heat transfer, while the difference is minor for friction factor. In order to estimate the level of time convergence of the results, the total simulation time is divided into four equally long parts that are averaged individually and where the dotted lines show the maximum and minimum of these averages. Since the variation in global mass flow when using constant pressure drop is relatively small, the variation in friction factor is smaller than for Nu. For the constant mass flow condition the friction factor is obtained by averaging a limited number of instant results, which is reasonable due to the small variation of the pressure drop. In addition it is also confirmed that the spurious low frequency content is only obtained using the smaller model sizes. To verify that the model size is sufficient, the higher Re case for CFL~1 was tested using L=4P and W=4.8H, which affected the results <1%.

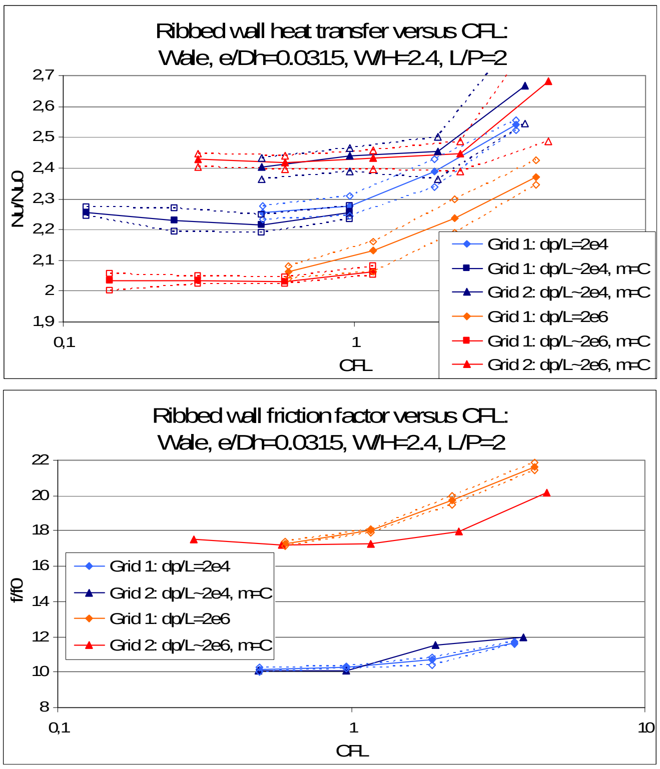

Figure 11: Ribbed wall heat transfer (top) and friction factor (bottom) for Wale SGS-model for different Re, grids and time steps. The dotted lines show max/min level.

Figure 12 shows the instant and averaged streamwise velocity field for different Re. The flow structure is similar, even though the negative velocity region behind the rib is stronger for higher Re. In addition the reattachment point is slightly upstream at higher Re, which is in accordance with [5] even though the difference is not large.

Figure 13 shows a summary of the RANS and LES results together with the correlations extrapolated to a wide channel and high Re. LES results using both Grid 1 and Grid 2 are shown, since the grid dependency should be the main source of error in the LES results, and the remaining error for Grid 2 should be small compared to the difference between the grids. Then the conclusion is that Nu is rather constant between Re=24k and 230k and that the LES results are quite similar to the correlation of Han [5]. For the friction factor LES predicts slightly higher values than both correlations and RANS.

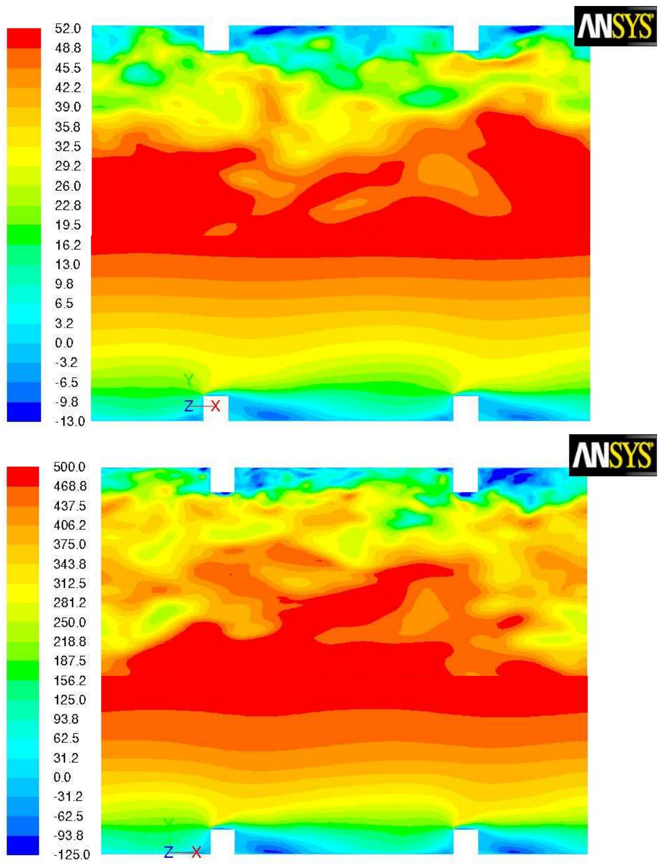

Figure 12: Instant (upper half) and averaged (lower half) streamwise velocity field for Re=24k (upper) and Re=230k (lower) for Grid 2, P/L=2, W/H=2.4 & CFL~1.

Table 4: Ribbed heat transfer for Grid 2, Re=230k, e/D$_h$=0.0315, L=2P, W=2.4H and CFL~1.

Case	Q	Properties	Nu/Nu0
Data as Table 1	10k	Constant	2.43
SGT-800 conditions	100k	Constant	2.40
SGT-800 conditions	100k	T dependent	2.39

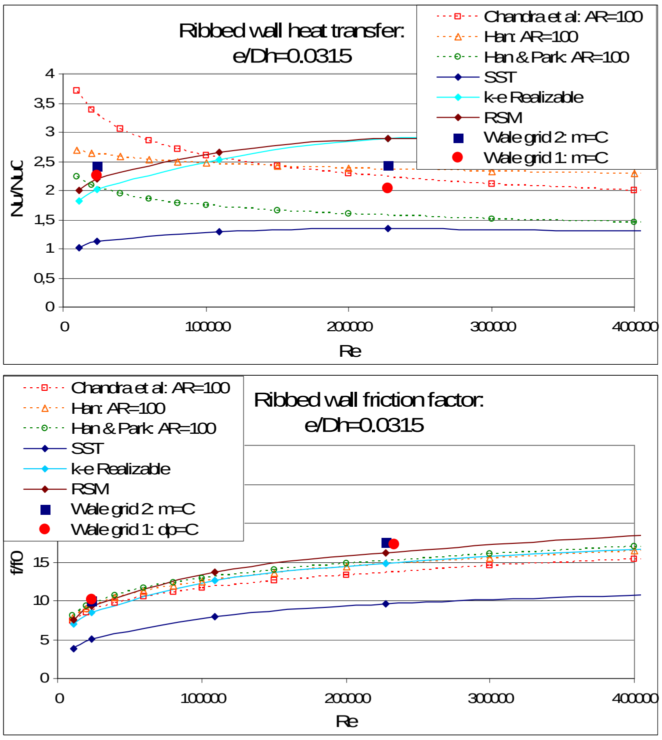

Figure 13: Ribbed wall heat transfer (top) and friction factor (bottom) for correlations, RANS and LES.

Apart from Re~230k, e/D$_h$~0.0315, P/e~10 and scaled to the correct dimensions, the prediction of SGT-800 liners include cooling air at ~700K and ~20bar, temperature dependent fluid properties and a temperature gradient between the wall and air bulk temperature of ~200K (here obtained by increasing the heat flux). Corresponding LES simulations as presented in Table 4 show that Nu compared to the previous test case is affected less than a couple of percent which is within the range of the time convergence. This shows that SGT-800 conditions or variable properties do not affect the results significantly.

CONCLUSIONS

The SGT-800 combustor liner rib cooling involves high Re of the order of 200k-300k, one sided 90 degree rib cooling in a wide channel of varying height, e/D$_h$~0.028-0.038, P/e~10, large temperature gradients affecting the fluid properties, conjugate heat transfer, corner sharpness defined by production tolerances and curved surfaces in both axial and tangential direction. The combined effect is not included in any empirical correlation found in the open literature and hence there is a need for complementary measurements or improved simulation accuracy. Due to the lack of accuracy for RANS simulations for 90 degree rib cooling there is a potential of using LES, if sufficient resolution and simulation time is used. In order to estimate the amount of required computational resources for a defined level of accuracy the introduced errors on the global parameters of Nu and friction factor have been estimated for different simplifications. These include simulation time, channel length and width, time step size, sub grid scale model and cell size.

The channel width showed large influence and the width must be larger than the channel height. However, additional width or increase size in streamwise direction affects the results less than a few percent. Simulations using small model sizes are often experiencing much more low frequency dynamics than the larger models, which therefore is assumed to be artificial dynamics due to the periodic boundary conditions. Therefore a model size of $L \geq 2P$ and $W \geq 2.4H$ is recommended, and then 10-20 flow through times is usually sufficient for converged statistics. The time step size was shown to be a minor factor as long as the global CFL<1, even though the maximum CFL is ~20 times larger. For larger time steps the error increases by 5-10% when doubling the time step.

The grid dependency investigation showed that the near wall resolution in between the ribs have large influence on the results, even though $y+<1$ was obtained. Therefore a second grid was created where $x+<50$ and $z+<30$ are obtained in this region, which resulted in acceptable grid independency i.e. ~4% when refining all cells. Therefore the total error in the simulations using Grid 2, due to time step, geometrical size and cell size, is estimated to <10% which is comparable to many experiments. A method for estimating the accuracy using CFD is important for the industry due to the common problem of extrapolating experimental data or correlations outside their valid ranges, since budget and lead time requirements do not permit experimental validation on a standard basis. However, the LES results agree well with the extrapolated correlation of Han [5], while the other extrapolated correlations deviate.

The investigation of SGT-800 engine conditions that apart from high Re includes high temperature gradients and temperature dependent fluid properties showed that these additional difficulties results in negligible effect on the heat transfer.

The next step is to apply this simulation strategy in order to extend the correlation ranges at high Re, such as e/D_h, P/e, curvature effects, rib shape etc in order to be applicable to SGT-800 conditions. Future topics also include measurements of the influence of the identified key parameters and/or further validation using another relevant case where there are accurate experimental data to verify the used method.

ACKNOWLEDGMENTS

The author would like to acknowledge Siemens Industrial Turbomachinery AB, Finspong, Sweden for the permission to publish this paper. Additionally the author acknowledges all Siemens employees involved in the development work during the concept, design and verification phases of the project.

REFERENCES

[1] SGT-800 information: http://www.energy.siemens.com/hq/en/power-generation/gas-turbines/sgt-800.htm

[2] Björkman M., Shukin S. & Annerfeldt M. *Siemens SGT-800 industrial gas turbine enhanced to 47MW. Design modifications and operation experience*, ASME GT2008-50087.

[3] Lörstad, D., Pettersson, J. & Lindholm, A. *Emission reduction and cooling improvements due to the introduction of passive acoustic damping in an existing SGT-800 combustor*. ASME GT2009-59313.

[4] Sundberg J. 2006. *Heat transfer Correlations for gas turbine cooling*. MSc thesis, University of Linköping, Sweden.

[5] Han J.C. 1988. *Heat transfer and friction characteristics in rectangular channels with rib turbulators*. J. Heat transfer 110 pp. 321-328.

[6] Han J.C. & Park J.S. 1988. *Developing heat transfer in rectangular channels with rib turbulators*. Int. J. Heat mass transfer. 31 pp. 183-195.

[7] Han J.C. Ou S., Park J.S and Lei C.K. 1989. *Augmented heat transfer in rectangular channels of narrow aspect ratios with rib turbulators*. Int. J. Heat mass transfer 32 pp. 1619-30.

[8] Chandra P.R., Niland M.E. & Han J.C. 1997. *Turbulent flow heat transfer and friction in a rectangular channel with varying numbers of ribbed walls*. J Turbomachinery 119 pp. 374-380.

[9] Rallabandi A.P., Yang H. and Han J.-C, 2009. *Heat transfer and pressure drop correlations for square channels with 45 deg ribs at high Re*. ASME J. Heat transfer 131-071703.

[10] Rallabandi A.P., Alkhamis N. and Han J.-C. *Heat transfer and pressure drop measurements for a square channel with 45deg round edged ribs at high Re*. ASME GT2009-59546.

[11] Kunstmann S., Wolfersdorf J. and Ruedel U. Heat transfer and pressure drop in combustor cooling channels with combinations of geometrical elements. ASME GT2010-23234.

[12] Hagari T., Ishida K., Oda T., Douura Y. and Kinoshita Y. Heat transfer and pressure losses of W-shaped small ribs at high Reynolds numbers for combustor liner. ASME GT2010-23197.

[13] Chen W., Ren J. and Jiang H. Verification of RANS for analyzing convective cooling system with and without ribs. ASME GT2009-59427.

[14] Zehnder F., Schüler M., Weigand B., von Wolfersdorf J. and Neumann S.O. The effect of turning vanes on pressure loss and heat transfer of a ribbed rectangular two-pass internal cooling channel. ASME GT2009-59482.

[15] Watanabe K. and Takahashi T. LES simulation and experimental measurement of fully developed ribbed channel flow and heat transfer. ASME GT2002-30203.

[16] Takahashi T. and Watanabe K. Large Eddy Simulation of the flow and heat transfer in a rectangular channel with crossed angles ribs. ASME GT2004-53673.

[17] Ahn J. Choi H. and Lee J.S. Large Eddy Simulation of the flow and heat transfer in a channel roughened by square or semicircle ribs. ASME GT2004-53401.

[18] Sewall E.A. and Tafti D.K. Large Eddy Simluation of the flow and heat transfer in the 180° bend region of a stationary ribbed gas turbine internal cooling duct. ASME GT2005-68518.

[19] Saha A.K. & Acharya S. Flow and heat transfer in an internally ribbed duct with rotation: An assessment of LES and RANS. ASME GT2003-38619.

[20] Tyagi M. and Acharya S. Large Eddy Simulations of the flow and heat transfer in rotating ribbed duct flows. ASME GT2004-53924.

[21] Fluent theory manual 12.1. www.fluent.com

